Atomic effective pseudopotentials for semiconductor nanostructures calculations

J.R. Cárdenas, and G. Bester

The main motivation for deriving atomic effective pseudopotentials (AEPs) relies on the computational savings that may be gained by circumventing the self-consistent optimization of the density, which is at the heart of density functional theory (DFT). The aim is thereby to address the omnipresent nanoscale, where the relevant structures include thousands, and often hundred thousands, of atoms. The philosophy behind an AEP, not only bypasses the need for a self-consistent solution, but also allows to focus on a selected part of the eigenvalue spectrum. The number of "bands" that scales with the number of atoms in DFT, is now independent of the system size. This latter characteristic is ideal for the study of optical properties or transport, where mainly the energy states around the band gap of the materials are involved.

Here we introduce a new generation of pseudopotentials that represent the scattering due to all the electrons. In this sense, it is distinct from the ionic pseudopotentials derived for DFT. We derive our atomic effective pseudopotentials via an analytic connection to the effective crystal potential from DFT. Our methodology is based on DFT where the central quantity is the effective Kohn-Sham potential $V^{\rm eff}$ that describes all the interactions of a single electron with its environment:

$$\left(-\frac{\hbar^2}{2m}\Delta + V^{\rm eff}(\mathbf{r})\right)\psi_i(\mathbf{r}) = \varepsilon_i\psi_i(\mathbf{r}), \tag{1}$$

$$V^{\rm eff}(\mathbf{r}) = V^{\rm ext}(\mathbf{r}) + V^{\rm Hartree}[n(\mathbf{r})] + V^{\rm xc}[n(\mathbf{r})],$$

where $n(\mathbf{r}) = \sum_i^{\rm occ} |\psi_i(\mathbf{r})|^2$ is the charge density of all occupied single-particle states ψ_i. The second key component is given by the transformation, following the frozen-core approximation, from the true Coulomb potential $V^{\rm ext}$ into a pseudopotential divided in a local ($V^{\rm psp,loc}$) an a non-local ($\widehat{V}^{\rm psp,nloc}$) part.

During the self-consistent cycle of the Kohn-Sham equations (Eq. 1) the density is updated until the ground state density $n^{\rm scf}$ is found. The starting point for the derivation of our AEPs is the local part of the self-consistent effective potential:

$$V^{\rm loc,eff}(\mathbf{r}) = V^{\rm psp,loc}(\mathbf{r}) + V^{\rm Hartree}[n^{\rm scf}(\mathbf{r})] + V^{\rm xc}[n^{\rm scf}(\mathbf{r})]. \tag{2}$$

The AEPs of a binary system cannot be directly extracted from the screened local effective potentials of DFT, but can be determined through $v_+ = v_a + v_c$ and $v_- = v_a - v_c$, where $v_a(v_c)$ stands for the anion (cation) potential. We start by explicitly dividing $V^{\rm loc,eff}(\mathbf{r})$ into cation and anion components, for systems with equal number of anions (N_a) and cations (N_c):

$$V^{(1)}_{\rm loc}(\mathbf{r}) = \sum_{i=1}^{N_a} v_a(\mathbf{r} - \boldsymbol{\tau}_i) + \sum_{j=1}^{N_c} v_c(\mathbf{r} - \boldsymbol{\tau}_j), \tag{3}$$

keeping the same atomic structure, and merely interchanging the atom types (index i and j), we rewrite:

$$V^{(2)}_{\rm loc}(\mathbf{r}) = \sum_{i=1}^{N_c} v_c(\mathbf{r} - \boldsymbol{\tau}_i) + \sum_{j=1}^{N_a} v_a(\mathbf{r} - \boldsymbol{\tau}_j). \tag{4}$$

The potentials $V^{(1)}_{\rm loc}$ and $V^{(2)}_{\rm loc}$ are obtained for structures with the same atomic positions $\boldsymbol{\tau}$, but with an inverted occupation of cations and anions. By adding and subtracting $V^{(1)}_{\rm loc}$ and $V^{(2)}_{\rm loc}$ we find:

$$V^{(1\pm2)}_{\rm loc}(\mathbf{r}) = V^{(1)}_{\rm loc}(\mathbf{r}) \pm V^{(2)}_{\rm loc}(\mathbf{r}) = \sum_{n=1}^{N_{atoms}} v_{\pm}(\mathbf{r} - \boldsymbol{\tau}_n). \tag{5}$$

The Fourier transform of the last two equations leads to the relations:

$$V^{(1\pm2)}_{\rm loc}(\mathbf{G}) = \frac{1}{\Omega}\int_\Omega e^{i\mathbf{G}\cdot\mathbf{r}} V^{(1\pm2)}_{\rm loc}(\mathbf{r})d\mathbf{r} = \frac{1}{\Omega}\left[\sum_{n=1}^{N_{atoms}} (\pm1)^{n+1} e^{i\mathbf{G}\cdot\boldsymbol{\tau}_n}\right] v_{\pm}(\mathbf{G}). \tag{6}$$

The potentials $v_+(\mathbf{G})$ and $v_-(\mathbf{G})$ are complex quantities, but into the scheme of the spherical approximation used in this work, only the real part of the atomic potentials is of interest. We can extract the spherically averaged AEPs from Eqs. (6), by separating them into their real and imaginary components, and write:

$$v_{\pm}^{\mathrm{SA}}(|\mathbf{G}|) = Re[v_{\pm}(\mathbf{G})] = \Omega \left[\frac{Re[V_{\mathrm{loc}}^{(1\pm2)}(\mathbf{G})]}{\beta_{\pm}} + \frac{Im[V_{\mathrm{loc}}^{(1\pm2)}(\mathbf{G})]}{\alpha_{\pm}} \right] \left(\frac{\beta_{\pm}\alpha_{\pm}}{\beta_{\pm}^2 + \alpha_{\pm}^2} \right), \tag{7}$$

where

$$\beta_{\pm} = \sum_{n=1}^{N_{atoms}} (\pm 1)^{n+1} \sin(\mathbf{G} \cdot \boldsymbol{\tau}_n), \qquad \alpha_{\pm} = \sum_{n=1}^{N_{atoms}} (\pm 1)^{n+1} \cos(\mathbf{G} \cdot \boldsymbol{\tau}_n). \tag{8}$$

With $v_{\pm}^{\mathrm{SA}}(G)$ we can obtain the atomic potentials via $v_a = \frac{1}{2}(v_+ + v_-)$ and $v_c = \frac{1}{2}(v_+ - v_-)$ in $\mathbf{G}$-space.

To generate the atomic potentials, we used a zincblende structure made of 24 atoms and elongated along the [100] direction, regardless of the ground state structure of the different binary systems (wurtzite (wz), zincblende (zb) or rocksalt (rs)). We apply a compressive and a tensile deformation of 5% along the slab direction in order to break the symmetry of the crystal and allow the extraction of the long range interaction.

The method allows the derivation of AEPs via an analytic connection to the effective crystal potential from DFT. The use of large and judiciously chosen slightly deformed supercells gives us access to the long range response of the potential. We therefore derive the pseudopotentials on a very dense grid of $\mathbf{G}$ vectors, including both, the long and short range interaction regimes. The method is free of parameters and does not involve any fitting procedure and is as *ab initio* as the underlying DFT calculations. This simplicity allows us to generate, with a minimum of effort, unique (for a certain DFT norm-conserving pseudopotential) AEPs. We have successfully generated AEPs for 20 compound semiconductor materials [1,2]. A comparison between the results of our code LATEPP using our AEPs and DFT shows differences for the bulk calculations in the order of a few tens of meV, which originates from our spherical approximation of the local part of the potential.

We selected one III-V, one II-VI and one group IV material, namely AlP, ZnSe and SiC, and studied the band gaps under different strain conditions. We start by studying the bulk materials under the effects of uniform expansion and compression and show the results in Fig. 1. The AEP results follow well the self consistent DFT calculations. The deviations become important when the effective potential starts to be significantly modified by self-consistent effects. Until around 5% the approximation of rigid overlapping potentials remains accurate. The value of 5% is very large for a hydrostatic deformation and will not be encountered in any experimental situation.

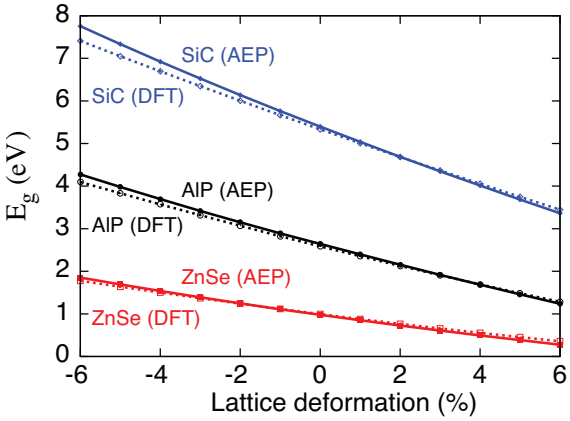

Figure 1: Bandgap for selected bulk materials, as a function of the lattice constant deformation calculated using self-consistent DFT and using our AEPs.

Until now, the AEPs were derived from DFT calculations of periodically repeated simulation cells of one material. We incorporate the effects of band-offsets in our AEPs by linking them together using DFT calculations of heterostructures. The procedure involves the interchange of the cation anion positions within a QW heterostructure formed by two slabs of different materials (A and B). The local potentials can be written as

$$V_{\mathrm{loc}}^{(1)}(\mathbf{r}) = \sum_{i=1}^{N_a^A} v_a^A(\mathbf{r} - \boldsymbol{\tau}_i) + \sum_{j=1}^{N_c^A} v_c^A(\mathbf{r} - \boldsymbol{\tau}_j) + \sum_{k=1}^{N_a^B} v_a^B(\mathbf{r} - \boldsymbol{\tau}_k) + \sum_{l=1}^{N_c^B} v_c^B(\mathbf{r} - \boldsymbol{\tau}_l), \tag{9}$$

$$V_{\mathrm{loc}}^{(2)}(\mathbf{r}) = \sum_{i=1}^{N_c^A} v_c^A(\mathbf{r} - \boldsymbol{\tau}_i) + \sum_{j=1}^{N_a^A} v_a^A(\mathbf{r} - \boldsymbol{\tau}_j) + \sum_{k=1}^{N_c^B} v_c^B(\mathbf{r} - \boldsymbol{\tau}_k) + \sum_{l=1}^{N_a^B} v_a^B(\mathbf{r} - \boldsymbol{\tau}_l). \tag{10}$$

Following the same procedure mentioned before, we can extract an expression for the real part of the potential for slab B ($v_{\pm}^{B}$)

$$Re[v_{\pm}^{B}(\mathbf{G})] = \frac{\Omega}{\alpha_{\pm}^{B}} Re[V_{\rm loc}^{(1\pm2)}(\mathbf{G})] - \frac{\alpha_{\pm}^{A}}{\alpha_{\pm}^{B}} Re[v_{\pm}^{A}(\mathbf{G})] + \frac{\beta_{\pm}^{B}}{\alpha_{\pm}^{B}} Im[v_{\pm}^{B}(\mathbf{G})] + \frac{\beta_{\pm}^{A}}{\alpha_{\pm}^{B}} Im[v_{\pm}^{A}(\mathbf{G})], \tag{11}$$

where $\beta_{\pm}$ and $\alpha_{\pm}$ are given by Eqs. (8), but restricted to each one of the slabs A or B. In the last equation, the imaginary components, which are basically the result of the deformation or loss of sphericity of the potentials due to the environment, vanish in most of the points and the expression simplify to

$$Re[v_{\pm}^{B}(\mathbf{G})] = \frac{\Omega}{\alpha_{\pm}^{B}} Re[V_{\rm loc}^{(1\pm2)}(\mathbf{G})] - \frac{\alpha_{\pm}^{A}}{\alpha_{\pm}^{B}} Re[v_{\pm}^{A}(\mathbf{G})]. \tag{12}$$

We now fix the AEPs of slab A to the potential derived from the bulk calculation and extract from the equation the potentials for slab B up to the value of $G = G_c$, the shortest G vector found in a two atoms cell. For values larger than G_c the linked and binary potentials are identical.

We test the long-range response of the AEPs due to the presence of a heterostructure interface. In Fig. 2a we plot the band gap as a function of the well (or barrier) thickness for a 36 atom [100] oriented A/B superlattice with zincblende structure. As test systems we select: GaP/AlAs, CdSe/ZnTe and Si/Ge.

In order to see the effects on the quality of the wave functions, we selected the GaP/AlAs supercell with 14 layers of GaP and 4 layers of AlP and show in Fig. 2b the square of the VBM and CBM wave functions after averaging over the (100) planes. We compare the AEP with the DFT state densities and notice a good agreement for the envelope of these strongly oscillating functions. Of relevance for the test is the fact that the long range response of the potentials are called upon to describe the long-range oscillations of the envelope functions and the asymmetry on the localization of the wave functions due to the different character of the interfaces, GaAs on one side and AlP on the other.

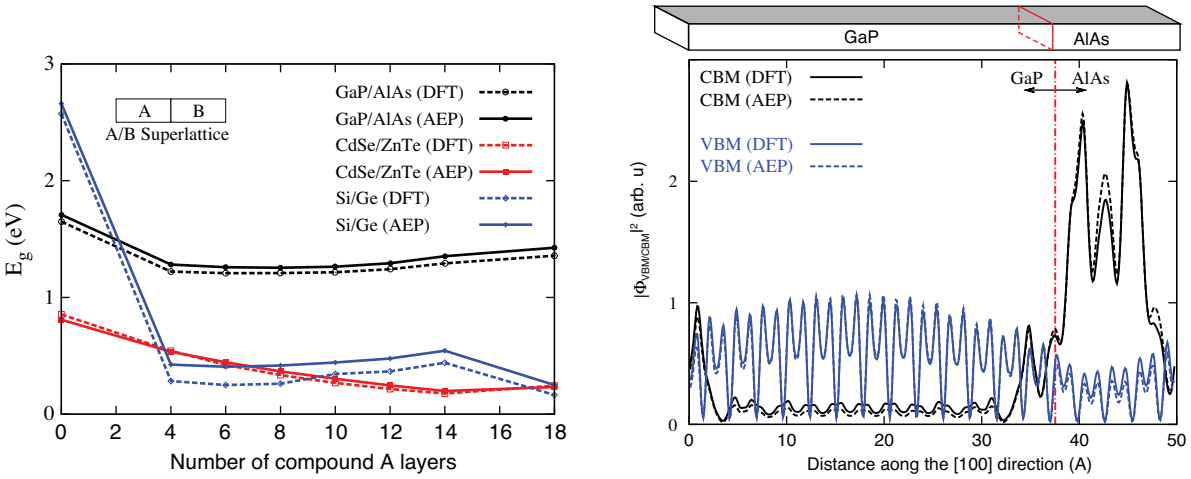

Figure 2: (a) DFT and AEP calculations for superlattices with 36 atoms along the [100] direction. The size of the wells and barriers are modified trough the variation of the proportion of the compound materials. (b) Square of the CBM and VBM wave functions in a [100] GaP/AlAs superlattice with 14 layers of GaP and 4 layers of AlP. The wave functions have been integrated in planes along the axes of the superlattice. The calculations are done using DFT and our AEPs.

In summary, we have developed a methodology to derived atomic effective pseudopotentials (AEPs) from simple DFT calculations. The procedure involves DFT calculations for two slabs with compressed and expanded regions. We establish an analytic connection between the DFT effective Kohn Sham potentials and the AEPs. The procedure is therefore free of parameters and does not involve any fitting procedure, which represents the main achievement of this work. We furthermore establish a method to connect the AEPs for different materials, rigorously from DFT calculations. Our AEPs intrinsically contain band-offsets between materials that are inherited from the DFT calculations, without having to explicitly calculate them. We demonstrate the accuracy and transferability of the AEPs for a total of 9 III-V, 6 II-VI and 5 group IV elements and find very good agreement with self-consistent DFT calculations.

References:

[1] *Cárdenas, J.R. and G. Bester* Physical Review B **86**, 115332 (2012).

[2] `http://www.fkf.mpg.de/bester/downloads/downloads.html`